UAV-based Environmental Monitoring using Multi-spectral Imaging

Martin De Biasio[a], Thomas Arnold[a], Raimund Leitner[a], Gerald McGunnigle[a], Richard Meester[b]

[a]CTR Carinthian Tech Research AG, Europastrasse 4/1 St. Magdalen, 9524 Villach, Austria;
[b]Quest Innovations B.V., Middenmeer, The Netherlands;

ABSTRACT

Monitoring the soil composition of agricultural land is important for maximizing crop-yields. Carinthian Tech Research, Schiebel GmbH and Quest Innovations B.V. have developed a multi-spectral imaging system that is able to simultaneously capture three visible and two near infrared channels. The system was mounted on a Schiebel CAMCOPTER® S-100 UAV for data acquisition. Results show that the system is able to classify different land types and calculate vegetation indices.

Keywords: multi-spectral imaging, vegetation, soil composition

1. INTRODUCTION

Soil monitoring is important for maximizing crop-yields. Accurate and up-to-date maps of water status, nutrient deficiencies and pest infestation allow farmers to take rapid, targeted action that minimizes costs and environmental impact. Manual monitoring involves taking ground samples and estimating the soil water status at random locations. For large areas this is time consuming and cost intensive, furthermore, it gives only a sparse sampling of the area.

Recently Unmanned Aerial Vehicles (UAV's) have become much more widely used and economic[3,5] Advances in imaging and computation have also made spectral imaging techniques more affordable. By combining these technologies, remote sensing techniques, which were previously limited to satellite-based or military systems, can now be economically applied to make frequent and high resolution surveys of agricultural land.

This article reports preliminary trials of a multi-spectral system mounted on an UAV. The UAV was flown over land containing various types of vegetation. The imaging system captured five bands (three in the VIS, two in the NIR) with a spatial resolution of approximately 10cm x 10cm. The image sequence was stitched together and the Normalized Difference Vegetation Index (NDVI) was calculated and used to classify each pixel in the image. The system was found to accurately classify land usage and we are currently working on a system to identify water stress in crops.

2. SPECTRAL IMAGING

Spectral Imaging (SI) is the combination of machine vision and spectroscopy.[2] SI acquires spatially resolved images of a measurement sample at different wavelengths and combines them into a three dimensional image cube. The two classical approaches for the acquisition of hyper-spectral image data are *wavelength scanning* and *spatial scanning*. Both methods have in common that it takes more than one integration time for the acquisition of a hyper-spectral image cube.

Further author information: (Send correspondence to Martin De Biasio E-mail: martin.debiasio@ctr.at, Telephone: 0043 4242 56300 224)

2.1 Spatial Scanning SI

Spatial scanning techniques use imaging spectrographs, e.g. prism-grating-prism combinations that disperse incident light of a single line of an object into its spectral components and project it onto a two dimensional sensor array. Fig. 1 illustrates the optical path of a *spatial scanning* system. Incident light from the sample is collected by an imaging lens. An entrance slit of the imaging spectrograph reduces the sample to a single line, which is dispersed with a special optic to a 2D image array. Hyper-spectral image data is generated by combining the scanned lines to a hyper-spectral image cube, see Fig. 2. The advantage of *spatial scanning* techniques is that it has a high spectral and spatial resolution.

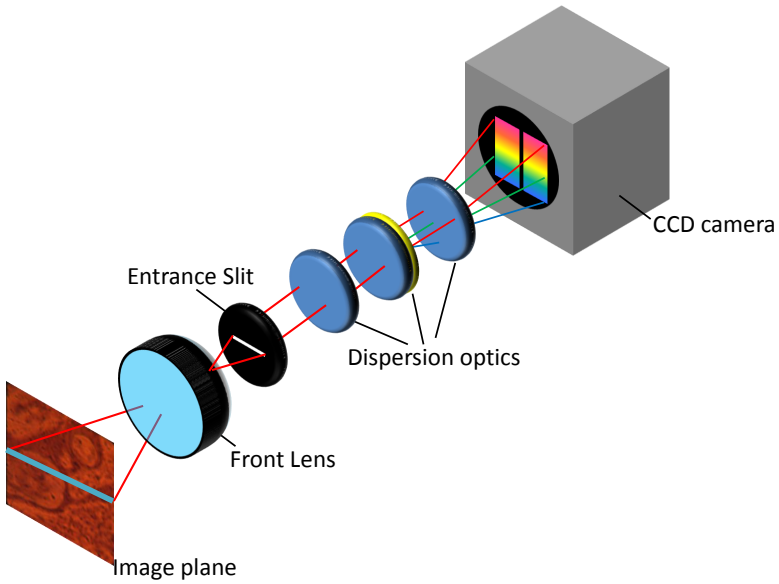

Figure 1. An imaging spectrograph (ImSpector, Specim, FI) disperses incident light of a single line of an object into its spectral components. Each image contains on the spatial axis the image line and the spectra of the pixels on the spectral axis. In consequence full spectral information for each image line of the target is available.[1]

2.2 Wavelength scanning SI

Wavelength scanning methods capture narrowband images sequentially. The spectral information is acquired sequentially. By combining the single narrow band monochrome images a hyper-spectral image cube is generated. One approach is to use interference bandpass filters mounted in a filter wheel. In this case the spectral information is limited to the number of filters that can be mounted in the filter wheel. The typical number of filters used is

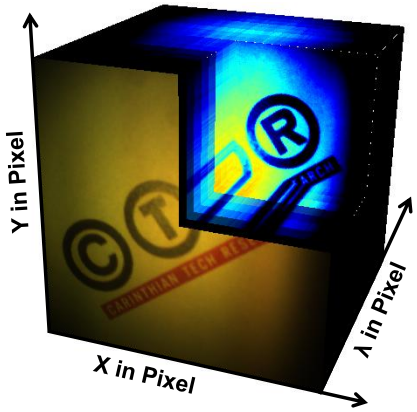

Figure 2. Hyper-spectral image cube consisting of a series of narrow band monochrome images.

between 6 to 12 filters. Tunable filters such as liquid crystal tunable filters (LCTF) or accousto-optical tunable filters (AOTF) allow a more flexible setup. The wavelength range within the filter specification can be controlled easily by a computer within μs to ms. The main disadvantage of *wavelength scanning* approaches is, that the sample needs to stay stationary during measurement or motion artefacts occur. If the sample is moving during the acquisition, image registration algorithms have to be applied to align the spectral information within the hyper-spectral image cube.

2.3 Multi-channel camera system

Multi-channel camera systems are a form of *wavelength scanning* approaches. Incoming light from a measurement sample is projected with specially designed dichroic coated prisms to single monochrome CCD arrays. The dichroic coating acts as a mirror with a reflectance value $> 98\%$, preventing the light losses that would occur with interference bandpass filters. The custom design prism reduces chromatic aberrations.

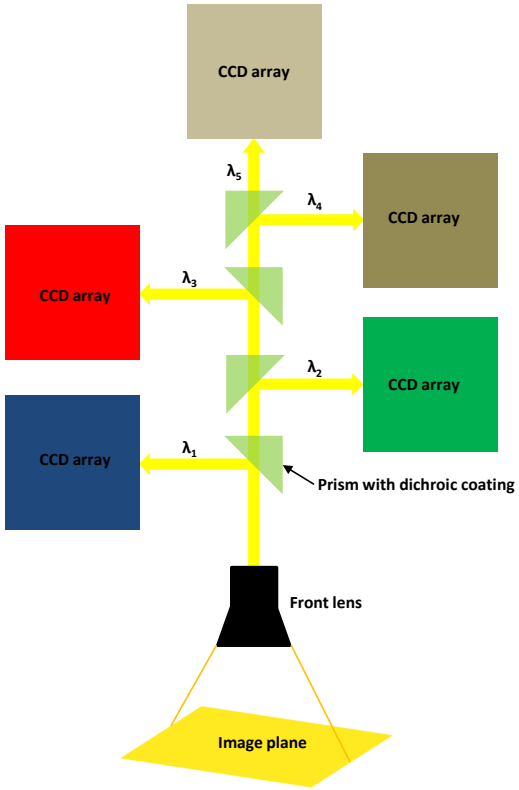

Figure 3. Optical design of the Quest Innovations B.V. 5 CCD multi-channel camera system.

The optical design of the system ensures that exactly the same image is projected onto each CCD array. When taking an image of a moving scene no registration of the single images is required.

Since this is an experimental design the front lens projects an image that is smaller than the sensor chips: this results in severe vignetting. Although this reduces the number of useable pixels, it does not affect the overall integrity of the system and future designs will overcome this problem.

3. DATA CAPTURE

The measurement setup for the presented work is shown in Fig. 4. We mounted a Condor-1000 MS5 5 CCD multi-channel camera (Quest Innovations B.V., The Netherlands) into the main payload port of a CAMCOPTER® S-100 (Schiebel, Vienna).

The camera is able to capture three VIS channels (400-500nm, 500-590nm and 590-670nm at 50% FWHM) and two NIR channels (670-850nm and 850-1000nm at 50% FWHM) concurrently. A fixed focus front lens was used. The weight of the additional technical equipment mounted on the UAV is a critical constraint. Therefore a low weight, shock resistant, embedded PC system V-Box 2 (NextSystem, Vienna) was attached to the side payload port.

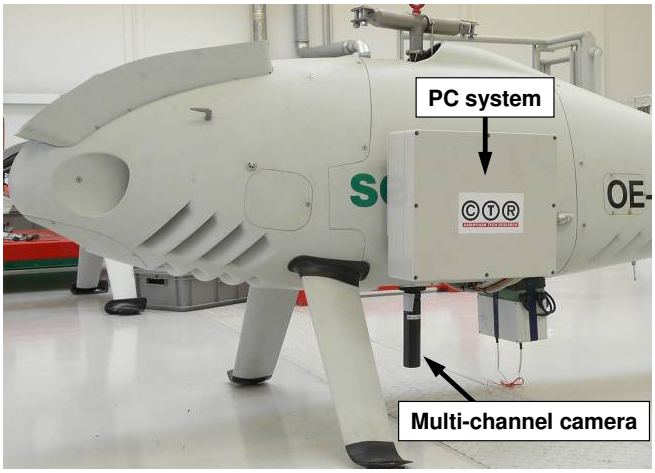

Figure 4. Multi-channel camera (Quest Innovations B.V., The Netherlands) mounted into the main payload of a CAMCOPTER® S-100 (Schiebel, Vienna). The embedded PC system is attached to the side payload port.

For the data acquisition the UAV followed a circular flightpath (approx. one mile circumference) over a partially snow covered area containing mixed vegetation, Figure 5. The data acquisition was started and stopped remotely by the pilot. Images where taken during the whole flight at flight altitudes varying from 150 to 500 feet.

Figure 5. The CAMCOPTER® S-100 hovering above the test area.

4. STITCHING THE IMAGES

The resulting data set consists of a sequence of 107 images each with 5 channels per circuit. Before the data can be analyzed and interpreted, it must be preprocessed so that the images of a sequence are combined with correct overlap and alignment. That is, the images must be stitched together into a larger mosaic image. The image channels correspond to different spectral bands; they have different optical paths within the camera and different optical transfer functions. Figure 6 shows a NIR image during flight at 810 nm (left) and 910 nm (right). For the aerial image we took NIR images at 910 nm. Images of this channel have a higher contrast and sharper edges

than the NIR images at 810 nm, which are blurred. For this reason, we based our stitching calculations on the 910nm image.

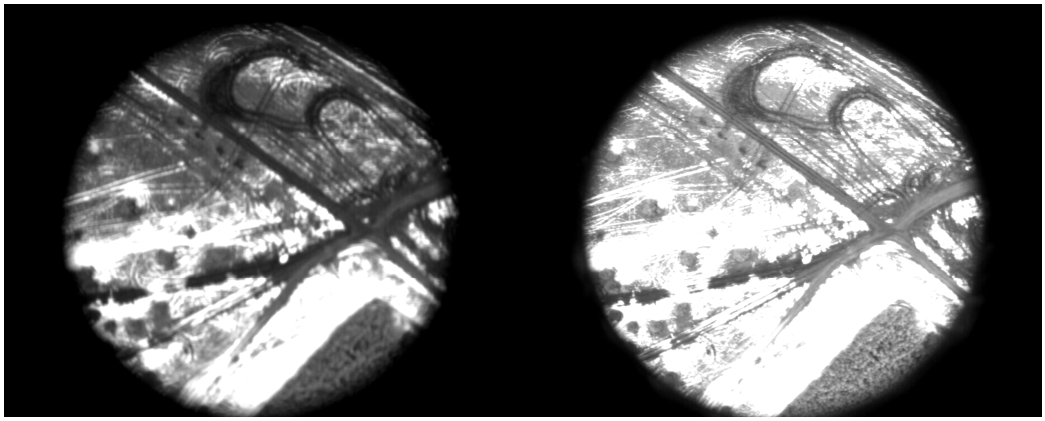

Figure 6. Example image captured with the UAV. The left hand image is taken with the 810 nm NIR image channel the image on the right side with the 910 nm NIR image channel. The forrest at the bottom right and the car tracks at the top show, that 810 nm image is blurred while the 910 nm NIR image is sharper at the same position.

The scheme of the registration algorithm is shown in 1. First the single images at 910 nm are loaded. The translations and rotations between the consecutive images are calculated. Each image is then transformed into a new coordinate system, and combined into a mosaic image. Depending on the amount of images the processing time can take up to a few minutes. For a post processing step this is not relevant, because a well matched aerial photo is generated. Figure 7 shows an aerial photo composed of 107 single images. The circular flight path of the helicopter can be seen. The dark region at the center of the mosaic image is an indirect consequence of vignetting and stitching. The raw image is cropped to remove the vignetted and blurred region at the image borders. This makes stitching far easier, but removes the (low quality) from the center of the mosaic image.

Algorithm 1 Scheme of registration algorithm

1: load single image from sequence
2: calculate translation and rotation
3: transform image
4: incorporate image into mosaic image using new coordinates

5. MEASURING VEGETATION

As a proof of concept we measured the Normalized Difference Vegetation Index (NDVI).[4] This is a standard coefficient, originally developed for LANDSAT images, that quantifies the presence of living vegetation in an image pixel. Leaves strongly absorb red light (from 600 to 700 nm), but strongly reflect near-infrared light (from 650 to 1100 nm). If there is much more reflected radiation in near-infrared wavelengths than in red wavelengths, then the vegetation in that pixel is likely to be dense and may contain some type of forest. The NDVI quantifies this observation in Equation 1. Our system relies on natural light: this may vary in intensity even over short time periods. Assuming that intensity variations affect both NIR and red bands the NVDI coefficient is robust to intensity variations.

$$NDVI = \frac{NIR - RED}{NIR + RED} \tag{1}$$

Our camera system has five detectors, three of which are sensitive to the wavelengths of light ranging from 400 to 700 nm and the other two detectors are sensitive to wavelengths ranging from 600 to 1000 nm. With this multi-spectral 5CCD detector it is possible to measure the intensity of light reflected by the Earth's surface

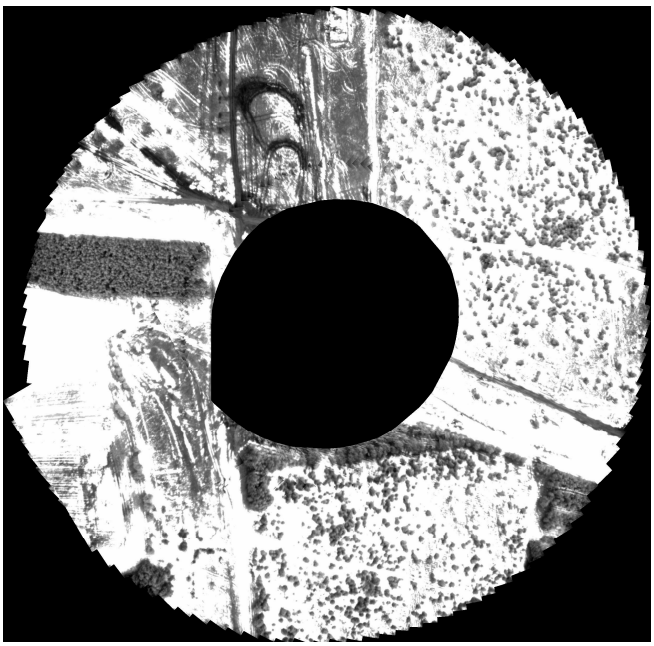

Figure 7. Aerial image composed of 107 single NIR images.

in visible and near-infrared wavelengths and quantify the photosynthetic capacity of the vegetation. With our imaging system, the RED term in Equation 1 stands for the red channel. The NIR terms stands for the average signal intensity in the wavelength range from 700 to 1000 nm. The NDVI for a given pixel result in a number in the range from -1 to $+1$. Where a value close to zero (0) means no vegetation and a value close to one ($+1$) indicates the highest possible density of green leaves. Since the images were acquired in the winter, deciduous plants can not be imaged. Snow cover also obscured a significant proportion of the vegetation. Despite these problems, the system was effective in classifying vegetation. Figure 8 shows two images segmented using the NVDI. It can be seen that trees are well differentiated from the other areas of the scene. In the left hand image even an unmetalled track can be separated from the background.

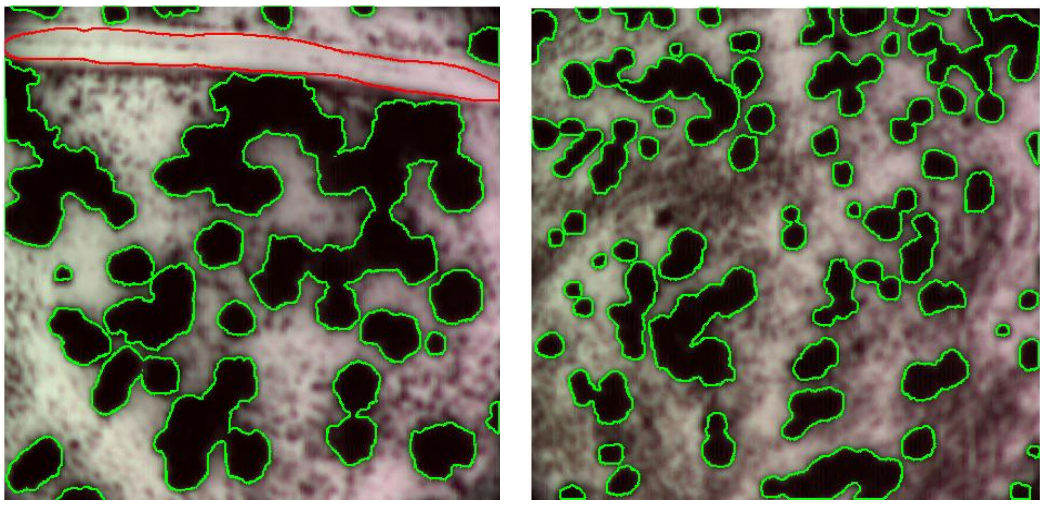

Figure 8. Segmentation result

6. DISCUSSION

This paper describes multi-spectral measurements made using a multi-channel CCD camera in combination with an UAV. Despite snow cover the system was effective in identifying the vegetation present. Future trials in the coming summer will allow the system to be tested over a wider range of plant species. Furthermore we plan to use spectral imaging techniques to identify spectral features that are related to water stress, nutrient deficiency and pest infestation. Once these bands have been identified, narrowband filters will be incorporated into the airborne system.

7. ACKNOWLEDGEMENT

The authors would like to express their gratitude to Quest Innovations B.V. and NextSytem Vertriebsges.m.b.H. for providing the hardware needed for the data acquisition. We would especially like to thank Schiebel GmbH for their flexibility, enthusiasm and willingness to help. Without their contribution this article would have not been possible.

REFERENCES

[1] T. Arnold, M. De Biasio, G. Lodron, and R. Leitner. Real-time spectral imaging system. In *Proceedings of 11th IASTED International Conference on Signal and Image Processing*, pages 276–281, 2009.

[2] G. H. Bearman, M. P. Nelson, and D. Cabib. *Spectral Imaging: Instrumentation, Applications, and Analysis.* SPIE-International Society for Optical Engine, 2000.

[3] J.A.J. Berni, P.J. Zarco-Tejada, L. Surez, V. Gonzlez-Dugo, and E. Fereres. Remote Sensing of Vegetation From UAV Platforms using Lightweight Multispectral and Thermal Imaging Sensors. *The International Archives of the Photogrammetry, Remote Sensing and Spatial Information Sciences*, XXXVII, 2008.

[4] A. J. Elmore, J. F. Mustard, S. J. Manning, and D. B. Lobell. Quantifying Vegetation Change in Semiarid Environments: Precision and Accuracy of Spectral Mixture Analysis and the Normalized Difference Vegetation Index. *Remote Sensing of Environment*, 73:87–102, 2000.

[5] S. Nebikera, A. Annen, M. Scherrer, and D. Oesch. A Light-Weight Multispectral Sensor for Micro UAV–Opportunities for Very High Resolution Airborne Remote Sensing. *The International Archives of the Photogrammetry, Remote Sensing and Spatial Information Sciences*, XXXVII:1193–2000, 2008.